Soft Matter

RSC Publishing

COMMUNICATION

View Article Online
View Journal | View Issue

Dynamics of force generation by confined actin filaments†

Cite this: *Soft Matter*, 2013, **9**, 2389

Received 3rd July 2012
Accepted 21st December 2012

DOI: 10.1039/c2sm26545a

www.rsc.org/softmatter

Xavier Banquy,[a] G. Wren Greene,[b] Bruno Zappone,[c] Anatoly B. Kolomeisky[d] and Jacob N. Israelachvili*[ab]

Forces generated by polymerizing/de-polymerizing actin filaments confined between two mica surfaces were measured using the Surface Forces Apparatus. The measurements show that confined actin filaments exhibit complex force-generation dynamics involving multiple "modes", the predominance of which is determined by the confinement gap and the applied force (confining pressure).

Force generation by filament-forming proteins like actin or tubulin has implications in many biological processes such as cell motility, vesicles trafficking or bacterial infection. Despite its importance, the physical–chemical mechanism underlying this phenomenon is still under active investigation. Single microtubule polymerization has been extensively used as a model system in many studies aiming to relate polymerization dynamics to force generation. Similar studies on single actin filaments are so far very scarce and have not reach statistical reliability yet. Measurements and theoretical studies of small bundles or arrays of actin filaments have shown that the polymerization rate of the filaments decreases exponentially with the applied normal force.[1–3] On the other hand many studies have reported force generation by actin filament networks using reconstituted (cross-linked) polymerizing medium or cytosolic extracts. So far there is no experimental data on force generation by large populations of independent (not crosslinked) actin filaments. Such studies are important to establish the interplay between structural plasticity, mechanical stresses, deformations and force generation dynamics.

We used the Surface Forces Apparatus (SFA)[4] to nucleate actin filaments at the contact point between two solid curved surfaces[5] and measure the forces they generate as a function of time. A 2 mg mL^{-1} solution of actin monomers in polymerizing buffer (5 mM Tris, 0.2 mM dithiothreitol and 0.2 mM ATP, pH 8) was injected between two atomically smooth mica surfaces, one of them being supported by a cantilever spring of stiffness 200 N m^{-1}. The separation distance D between the surfaces was monitored using Multiple Beam Interferometry (MBI). A video camera allowed following at 30 frames per second the fringes of equal chromatic order (FECO fringes) generated by a white light beam going through the two facing surfaces and resolved in a spectrometer. The distance D and the normal force F between the two mica surfaces could be resolved with an accuracy of 1 nm and 1 μN respectively.

After introducing the solution of actin monomers, the polymerization of actin monomers into filaments was triggered by confining the proteins in a small gap of 50 nm between the two mica surfaces for 10 min.[5] After this nucleation time, the surfaces were slowly separated at a constant speed of 10 nm s^{-1} and fluctuations in the FECO fringes position was continuously recorded. Post analysis of the FECO fringes allows calculating D and F as a function of time t. Fig. 1 (see also Fig SI-1† for more details) shows a typical set of experimental data obtained on separating the mica surfaces. The distance $D = 0$ corresponds to the separation distance of the mica surfaces at the end of the nucleation phase (*i.e.* 50 nm as mentioned before). The evolution of F as a function of D (or time t) can be divided into three main regimes. For $D = 0$–50 nm, F decays exponentially as D increases with a decay length of ≈62 nm (Fig. 1). This decaying regime corresponds to the elastic recovery of the compressed protein layers trapped between the two mica surfaces. As D is increased, a second regime develops where fluctuations in the separation distance start to appear. Fluctuations could be inhibited by addition of gelsolin, which acts as a capping agent, and phalloidin (see Fig. SI-2†) confirming that they were not a purely mechanical property of the actin network and were rather a consequence of a polymerization/depolymerization process. It is also important to note the mechanical displacement system of the SFA is stable (rigid, and mechanically vibration-isolated) enough to dampen

[a]*Department of Chemical Engineering, University of California at Santa Barbara, USA. E-mail: jacob@engr.ucsb.edu; Fax: +1 805-893-7870; Tel: +1 805-893-8407*
[b]*Materials Department, University of California at Santa Barbara, Santa Barbara, USA*
[c]*CNR-IPCF, UOS Cosenza, Università della Calabria, Rende (CS), Italy*
[d]*Department of Chemistry, Rice University, Houston, Texas 77005, USA*

† Electronic supplementary information (ESI) available. See DOI: 10.1039/c2sm26545a

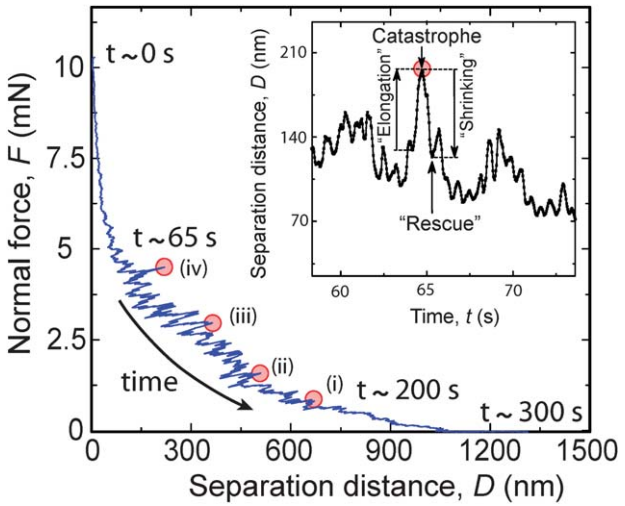

Fig. 1 Evolution of the normal force F as a function of the separation D between two mica surfaces bearing actin filaments generated by confinement induced nucleation. The data were recorded during separation of the surfaces at a constant speed of 10 nm s^{-1}. The fluctuations observed in the force profile are generated by the actin filaments growing and shrinking in the gap between the surfaces. The inset shows a short time window at $t \sim 65$ s where large fluctuations of D can be observed. (i)–(iv) refer to the positions at which the "static" measurements shown in Fig. 3 were obtained (see text for details).

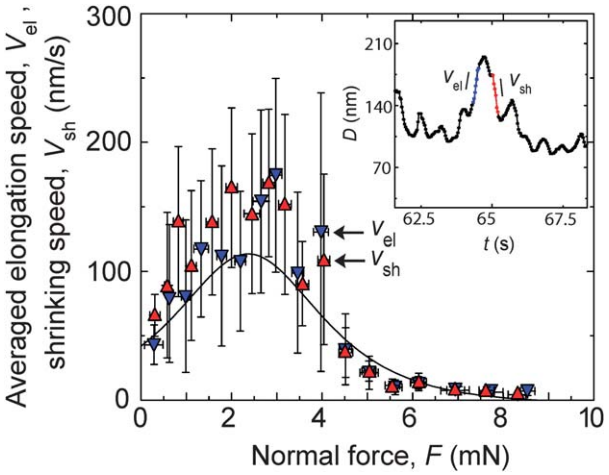

Fig. 2 Evolution of the average elongation, V_{el}, and shrinking speed, V_{sh}, as a function of the applied normal force, F. The results show two noticeably different regimes. For $F < 3$ mN, V_{el} and V_{sh} increase quasi linearly with F while for $F > 3$ mN both V_{el} and V_{sh} decrease exponentially with F. Error bars represent one standard deviation of 11 consecutive measurements. Note that the error bars decrease drastically in the second regime.

mechanical vibrations to less than 0.5 nm in buffer solution (see Fig SI-3†).

As we will see, the amplitude of these fluctuations varies with the average normal force $\langle F \rangle$ or average separation distance $\langle D \rangle$. These fluctuations can be described as elongation and shrinking events of the actin filaments associated to polymerization and depolymerization of the monomers. These fluctuations are similar to those reported for microtubules and are characterized by linear elongation or shrinking phases (see inset of Fig. 1) separated by catastrophe and rescue events.[6] Transitions from elongation to shrinking are generally sharp meaning that no apparent buckling of the filaments was observed.

Once the separation distance reaches a value of 850–900 nm, fluctuations of the separation distance D disappear and the interaction forces approach the detection limit. In this regime, the actin filaments grown from the two mica surfaces are far apart and barely touch each other. The elongation, V_{el}, and shrinking speeds, V_{sh}, were calculated from the slope of D *vs.* time t curve (see inset Fig. 1) with an experimental error of 4%. The experimental data shown in Fig. 2 were obtained by averaging $n = 11$ consecutive values of V_{el} or V_{sh} and the error bars represent the standard deviation associated to these mean values. These data can be divided into two main regimes. For F lower than 3 mN, V_{el} and V_{sh} are increasing with F, meaning that the dynamics (kinetics) of polymerization–depolymerization is accelerated by the normal force. Above a normal force of 3 mN, V_{el} decreases quasi exponentially. The data points in this regime can be logarithmically extrapolated to zero V_{el} in order to obtain an estimate of the stalling force, f_s. The value obtained by this procedure is 8 mN. Considering that the stalling force per actin filament is approximately 9 pN, this leads to approximately 8.8×10^8 filaments holding the external normal force. If these filaments were growing in a close packed configuration from the surfaces, then the minimum surface coverage of each filament would be approximately 7×7 nm^2, corresponding to a total area of 4.18×10^{-9} m^2 (equivalent to a disc of radius 36.5 μm).

The results in Fig. 2 present several important features. The first one is that V_{el} and V_{sh} are, on average, equal. More interestingly, the data shows that V_{sh} does depend on the normal force contrary to what many chemical–mechanical models have hypothesized so far.[7] Another important feature is the existence of a maximum in the velocity–force curve located at a normal force of 3 mN. The presence of a maximum in the velocity–force curve has been predicted by multiple-states models[8,9] but has never been experimentally confirmed. Fig. 2 also shows a fitted curve of the two-state model recently reported[8,9] using reasonable experimental parameters found in the literature (see Fig. SI-4 ESI† for more information about the model and the fitting results).

The low load regime of the velocity–force curve shown in Fig. 2 is characterized by very large fluctuations in V_{el} and V_{sh} values which contribute to increase the standard deviations associated to V_{el} and V_{sh} as represented in Fig. 2. The existence of these large fluctuations is not related to experimental errors but is rather a consequence of the appearance of different "populations" or "modes" of actin filaments exhibiting different polymerization dynamics. In order to further characterize this phenomenon, we ran "static" experiments where the average separation distance $\langle D \rangle$ (and therefore $\langle F \rangle$) was fixed while monitoring the time evolution of D.

The distribution function of V_{el} and V_{sh} are presented in Fig. 3 at four different $\langle D \rangle$ (or $\langle F \rangle$). The experimental distribution functions were fitted with Gaussian distributions as shown in Fig. 3. The choice of a Gaussian distribution was arbitrary but appears to give satisfactory (consistent and reproducible) fits to

the experimental data (R^2 between 0.85 and 0.95) for the data shown in Fig. 3(ii) to (iv). The data in Fig. 3(i) were poorly approximated by a double Gaussian distribution ($R^2 < 0.75$) which may indicate that other modes or multiple distributions might give better fits to the experimental data.

Independently of $\langle D \rangle$, V_{el} and V_{sh} exhibit a first peak at 50 ± 10 nm s^{-1}. As $\langle D \rangle$ was increased, V_{el} and V_{sh} distributions present a significant broadening which can be fitted by multi modal distribution curves. As $\langle D \rangle$ was increased, a second and third peak appear at $\langle V_{el} \rangle$, $\langle V_{sh} \rangle = 100 \pm 20$ nm s^{-1} and 170 ± 20 nm s^{-1}.

The results of Fig. 3 show that the large standard deviations in the elongation and shrinking rates observed in the dynamic experiment shown in Fig. 2 are due to the appearance of multiple *discrete* dynamic "modes". Most importantly, the quantized, *i.e.* discrete and non-independent, values obtained for $\langle V_{el} \rangle$ and $\langle V_{sh} \rangle$ at fixed $\langle D \rangle$ suggest that these modes emerge from a cooperative behaviour of the filament dynamics.

The origin of this cooperative behaviour is still unknown. The different distributions reported in Fig. 3 represent a time-averaged picture of the polymerization dynamics of the confined filaments over several minutes. As shown in Fig. 4A and B, the instantaneous evolution of the three parameters D, V_{el} and V_{sh} present an unexpected behaviour. The results clearly show that all three parameters increase and decrease

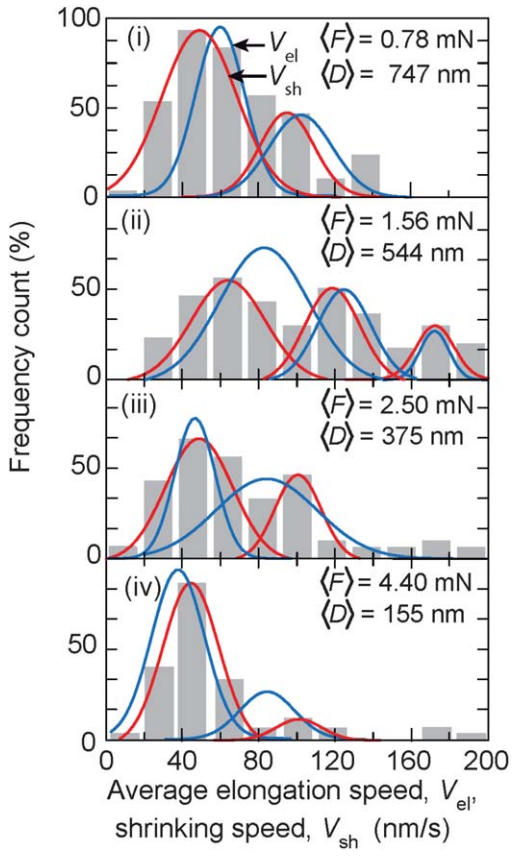

Fig. 3 Distributions of V_{el} and V_{sh} of actin filaments confined between two mica surfaces under constant normal force $\langle F \rangle$ and separation distance $\langle D \rangle$. For clarity, experimental data (shown as grey bars diagram) are shown only for V_{sh} (see Fig. SI-5A and B in ESI† for complementary graphs). Lines represent Gaussian distributions that were fitted to the experimental data.

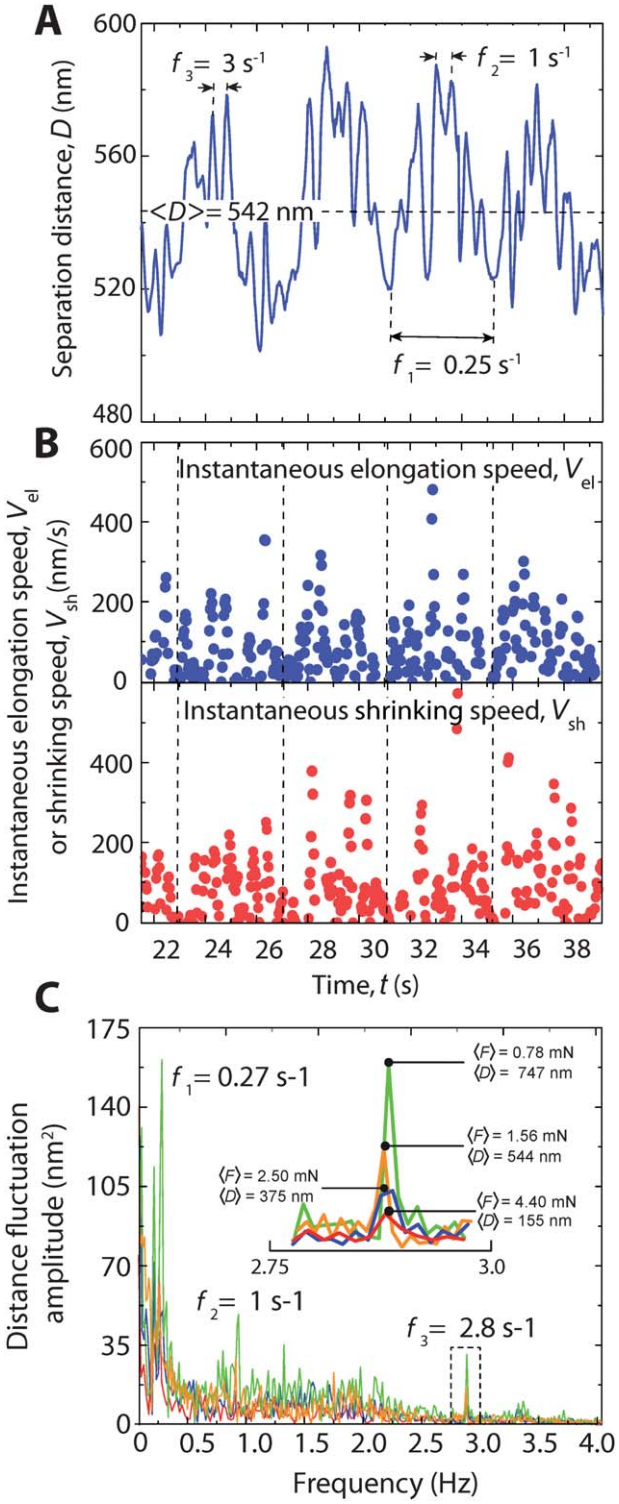

Fig. 4 (A) Evolution of the separation distance D with time showing periodic oscillations exhibiting three characteristic frequencies. (B) The corresponding evolution of V_{el} and V_{sh} as a function of time shows periodic switching of the filaments from a dormant state where the velocities are very low to an active state where they reach very high values. (C) The Fast Fourier Transform of D exhibit three main characteristic frequencies independently of $\langle F \rangle$ or $\langle D \rangle$ (each color corresponding to one different $\langle D \rangle$ or $\langle F \rangle$ (similar to the values presented in Fig. 3). In contrast, the distance fluctuation amplitude associated to these frequencies are strongly dependent on $\langle F \rangle$ or $\langle D \rangle$ (see inset).

periodically and synchronously. The main frequency of this periodic growth and shrinking of the filaments was assessed by performing a Fast Fourier Transform of D. As can be seen in Fig. 4C, the Fourier spectra present three characteristic frequencies $f_1 = 0.27\ s^{-1}$, $f_2 = 1\ s^{-1}$ and $f_3 = 2.8\ s^{-1}$ whose associated amplitudes decreases with $\langle D \rangle$ or $\langle F \rangle$. Other characteristic frequencies were also observed but did not present any clear or reproducible dependence with $\langle D \rangle$. The time evolution of V_{el} and V_{sh} shown in Fig. 4B clearly suggest that the filament polymerization dynamics periodically alter between an "active" state where V_{sh} and V_{el} can have very high values and a "dormant" state where the dynamics is almost stalled. This periodic increase in activity has been reported in different systems like neutrophils[10] and *Listeria monocytogenes*[11,12] and therefore seems to be a characteristic of the actin filaments only and not from their medium or associated proteins as often assumed.

A microscopic description of the velocity and displacement oscillations of actin propelled obstacles or surfaces was recently proposed.[13] In this model, filaments in the brush like conformation can exist in either compressed state or tensile state. This formalism seems to be close to our experimental conditions, except that in our case an additional restoring force from the cantilever spring needs to be considered. It is interesting to note that the value of the velocities obtained in our experiments are very similar to those reported by Gerbal *et al.*[12] for *Listeria* mutant but are on average 2 to 10 times smaller to those reported in bead motility assays in reconstituted medium.[14,15]

The time period between each increase of displacement speed is also very different in our study (a few seconds at most) compared to what was reported in these studies (5 to 10 minutes on average). Those discrepancies can be explained by the large difference in the surface curvatures of the two systems[14] (2 cm in our system compared to a few microns in most motility assays on beads or bacteria), and considering that the attachment dynamics of the filaments to the surfaces are also very different (not protein mediated in our case).[13]

All together, our results suggest that different "populations" of actin filaments each exhibiting a particular polymerization dynamics coexist and interact together to give rise to the emergence of a cooperative behaviour. There is an increasing amount of evidence that free actin filaments can have many different internal structural arrangements of the monomers[16,17] giving rise also to different mechanical properties and polymerization dynamics of the filaments.[18]

The two state model recently proposed by Fisher and Kolomeisky is, to our knowledge, the only one able to reproduce the observed non-monotonic dependence of the polymerization/depolymerization rates with the applied force. Unfortunately, this model does not predict the existence of different populations of filaments and therefore only describes an average statistical behaviour of the total system. It also does not consider any loading history effect on the dynamics of the filaments which can have an important impact on the filament dynamics.[19] Recently we reported[5] a two state mechanical model of the compressed actin filaments able to explain qualitatively the capacity of force amplification of actin filaments under cyclic compression–decompression. Therefore it is possible that the multiple dynamic modes observed in the present experiments arise from structural forms of different actin filaments exhibiting different polymerization–depolymerization kinetics, the predominance of each being determined by the applied normal force. Such argument could not only explain the force dependence of actin filament dynamics but also its dependence on the load history.

Notes and references

1 C. Brangbour, O. du Roure, E. Helfer, D. Demoulin, A. Mazurier, M. Fermigier, M. F. Carlier, J. Bibette and J. Baudry, *PLoS Biol.*, 2011, **9**, e1000613.
2 Y. Marcy, J. Prost, M. F. Carlier and C. Sykes, *Proc. Natl. Acad. Sci. U. S. A.*, 2004, **101**, 5992–5997.
3 K. Tsekouras, D. Lacoste, K. Mallick and J. Joanny, *New J. Phys.*, 2011, **13**, 103032.
4 J. Israelachvili, Y. Min, M. Akbulut, A. Alig, G. Carver, W. Greene, K. Kristiansen, E. Meyer, N. Pesika, K. Rosenberg and H. Zeng, *Rep. Prog. Phys.*, 2010, **73**, 036601.
5 G. W. Greene, T. H. Anderson, H. Zeng, B. Zappone and J. N. Israelachvili, *Proc. Natl. Acad. Sci. U. S. A.*, 2009, **106**, 445–449.
6 D. K. Fygenson, E. Braun and A. Libchaber, *Phys. Rev. E: Stat. Phys., Plasmas, Fluids, Relat. Interdiscip. Top.*, 1994, **50**, 1579–1588.
7 J. Howard, *Mechanics of Motor Proteins and the Cytoskeleton*, Sinauer Associates, Inc., Sunderland, 2001.
8 M. E. Fisher and A. B. Kolomeisky, *Physica A*, 1999, **274**, 241–266.
9 M. E. Fisher and A. B. Kolomeisky, *Proc. Natl. Acad. Sci. U. S. A.*, 1999, **96**, 6597–6602.
10 M. P. Wymann, P. Kernen, T. Bengtsson, T. Andersson, M. Baggiolini and D. A. Deranleau, *J. Biol. Chem.*, 1990, **265**, 619–622.
11 S. C. Kuo and J. L. McGrath, *Nature*, 2000, **407**, 1026–1029.
12 F. Gerbal, P. Chaikin, Y. Rabin and J. Prost, *Biophys. J.*, 2000, **79**, 2259–2275.
13 A. Gholami, M. Falcke and E. Frey, *New J. Phys.*, 2008, **10**, 033022.
14 A. Bernheim-Groswasser, J. Prost and C. Sykes, *Biophys. J.*, 2005, **89**, 1411–1419.
15 L. Trichet, O. Campas, C. Sykes and J. Plastino, *Biophys. J.*, 2007, **92**, 1081–1089.
16 V. E. Galkin, A. Orlova and E. H. Egelman, *Curr. Biol.*, 2012, **22**, R96–R101.
17 H. Y. Kueh and T. J. Mitchison, *Science*, 2009, **325**, 960–963.
18 H. Y. Kueh, W. M. Brieher and T. J. Mitchison, *Proc. Natl. Acad. Sci. U. S. A.*, 2008, **105**, 16531–16536.
19 S. H. Parekh, O. Chaudhuri, J. A. Theriot and D. A. Fletcher, *Nat. Cell Biol.*, 2005, **7**, 1219–1223.

